Nonlinear response function for time-domain and frequency-domain four-wave mixing

Shaul Mukamel and Roger F. Loring

Department of Chemistry, The University of Rochester, River Station, Rochester, New York 14627

Received September 20, 1985; accepted November 19, 1985

A unified theory of time-domain and frequency-domain four-wave mixing processes, which is based on the nonlinear response function $R(t_3, t_2, t_1)$, is developed. The response function is expressed in terms of the four-point correlation function of the dipole operator $F(\tau_1, \tau_2, \tau_3, \tau_4)$ and is evaluated explicitly for a stochastic model of line broadening that holds for any correlation time of the bath. Our results interpolate between the fast-modulation limit, in which the optical Bloch equations are valid, and the static limit of inhomogeneous line broadening. As an example of the relationship between time-domain and frequency-domain four-wave mixing, we compare the capabilities of steady-state and transient coherent anti-Stokes Raman spectroscopy experiments to probe the vibrational dynamics in ground and excited electronic states.

1. INTRODUCTION

Four-wave mixing (4WM) processes play an important role in current studies of nonlinear optical phenomena.[1-4] The most general 4WM process involves the interaction of three laser fields with wave vectors $\mathbf{k}_1$, $\mathbf{k}_2$, and $\mathbf{k}_3$ and frequencies ω_1, ω_2, and ω_3, respectively, with a nonlinear medium. A coherently generated signal with wave vector $\mathbf{k}_s$ and frequency ω_s is then detected (Fig. 1), where

$$\mathbf{k}_s = \pm\mathbf{k}_1 \pm \mathbf{k}_2 \pm \mathbf{k}_3 \tag{1a}$$

and

$$\omega_s = \pm\omega_1 \pm \omega_2 \pm \omega_3. \tag{1b}$$

Equations (1) imply that $\mathbf{k}_s$ and ω_s are given by any linear combination of the applied wave vectors and frequencies. The various types of 4WM processes differ according to the particular choices of $\mathbf{k}_s$ and ω_s [i.e., the particular choice of signs in Eqs. (1)]. They also differ according to the temporal characteristics of the applied fields. In one limit the applied fields (and the signal field) are stationary (S4WM).[5-13] In the opposite limit the applied fields are infinitely short pulses, resulting in an ideal time-domain 4WM (T4WM). Examples of T4WM experiments are photon echoes,[14-17] transient gratings,[18-24] and time-resolved coherent Raman scattering.[25-32] Realistic pulsed experiments involving pulses with finite duration are characterized by a finite spectral and temporal resolution and are intermediate between these two ideal frequency-domain and time-domain limits. The various 4WM experiments are often interpreted using different terminologies, and the relationships among these techniques are not always obvious. In this paper we present a unified framework for the interpretation of any 4WM process. The key quantity in the present formulation is the nonlinear response function $R(t_3, t_2, t_1)$, which contains all the microscopic information relevant for any type of 4WM. In Section 2 we introduce the nonlinear response function R and derive the general expression for 4WM. The two ideal limiting cases of time-domain experiments (T4WM) and frequency-domain 4WM (S4WM) are derived from the same unified expression. The nonlinear susceptibility $\chi^{(3)}$ that is commonly used in S4WM is also obtained in terms of R. In Section 3 we calculate the response function for a specific model system for molecular 4WM. The model consists of two manifolds of levels coupled to a thermal bath that causes dephasing. In Section 4 we present new expressions for the response function and $\chi^{(3)}$ for a stochastic model in which the thermal bath has a finite time scale. This model includes the model of Section 3 as a special case and interpolates continuously between the homogeneous (fast-modulation) and inhomogeneous (static) broadening limits. In Section 5 we focus on coherent anti-Stokes Raman spectroscopy (CARS). The T4WM and S4WM are compared in detail. The different roles of ground-state and excited-state resonances are analyzed. In Section 6 we summarize these results.

2. THE NONLINEAR RESPONSE FUNCTION FOR FOUR-WAVE MIXING

We consider a nonlinear medium interacting with a classical external electromagnetic field through the dipolar interaction. The total Hamiltonian of the system is

$$H_T = H + H_{\text{int}}. \tag{2}$$

Here H is the Hamiltonian for the material system in the absence of the radiation field. H_{int} represents the radiation–matter interaction and is given by

$$H_{\text{int}}(t) = \sum_{\alpha} E(\mathbf{r}_\alpha, t) V_\alpha, \tag{3}$$

where V_α is the dipole operator of the particle labeled α and located at $\mathbf{r}_\alpha$, and the summation is over all the molecules in the nonlinear medium. $E(\mathbf{r}, t)$ is the external electric field that for a general 4WM process (Fig. 1) can be decomposed into three components:

$$E(\mathbf{r}, t) = \sum_{j=1}^{3} [E_j(t)\exp(i\mathbf{k}_j \cdot \mathbf{r} - i\omega_j t) + E_j^*(t)\exp(-i\mathbf{k}_j \cdot \mathbf{r} + i\omega_j t)]. \tag{4}$$

0740-3224/86/040595-12$02.00

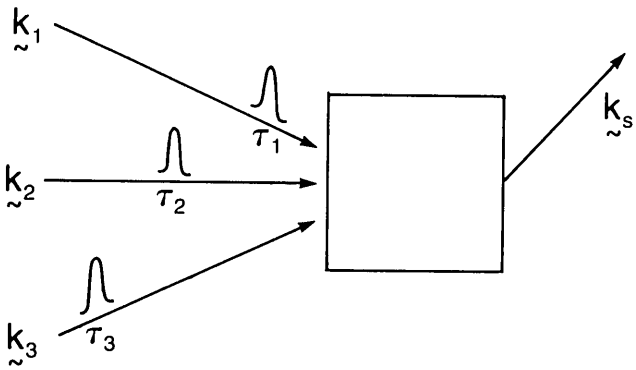

Fig. 1. The general 4WM process. The coherent signal with wave vector $\mathbf{k}_s$ is generated by a nonlinear mixing of the applied fields with wave vectors $\mathbf{k}_1$, $\mathbf{k}_2$, and $\mathbf{k}_3$.

We shall now adopt a simple model in which the active nonlinear medium consists of noninteracting absorbers and a set of bath degrees of freedom that interact with the absorbers but not with the electromagnetic field. In this case we can focus on one absorber located at $\mathbf{r}$ and write

$$H_{\text{int}}(t) = E(\mathbf{r}, t)V, \tag{5}$$

where V is the dipole operator of that absorber.

In order to calculate the 4WM signal, we start at $t = -\infty$ and assume that the system is in thermal equilibrium with respect to H (without the radiation field)

$$\rho(-\infty) = \exp(-\beta H)/\text{Tr}\exp(-\beta H), \tag{6}$$

where $\beta = (kT)^{-1}$. The system then evolves in time according to the Liouville equation

$$\frac{d\rho}{dt} = -i[H, \rho] - i[H_{\text{int}}, \rho]. \tag{7}$$

In Liouville-space notation,[33]

$$\frac{d\rho}{dt} = -iL\rho - iL_{\text{int}}\rho. \tag{8}$$

The action of the Liouville operator on an ordinary (dyadic) operator A is given by

$$LA \equiv [H, A], \tag{9a}$$

$$L_{\text{int}}A \equiv [H_{\text{int}}, A]. \tag{9b}$$

In Eqs. (7)–(9) and in the rest of this paper, we set $\hbar = 1$. We also define

$$\mathcal{V}A \equiv [V, A]. \tag{9c}$$

We shall be interested in calculating the polarization $P(\mathbf{r}, t)$ at position $\mathbf{r}$ at time t. This is given by the expectation value of the dipole operator V:

$$P(\mathbf{r}, t) \equiv \langle\langle V|\rho(t)\rangle\rangle, \tag{10}$$

where we are using the double-angle-bracket notation[33] to denote an inner product of operators. For any two operators,

$$\langle\langle A|B\rangle\rangle \equiv \text{Tr}(A^{\dagger}B). \tag{11a}$$

We shall also define a Liouville-space matrix element by

$$\langle\langle A|L|B\rangle\rangle \equiv \text{Tr}(A^{\dagger}LB). \tag{11b}$$

For a 4WM process we calculate $\rho(t)$ perturbatively to third order in L_{int}. We then get

$$P(\mathbf{r}, t) = (-i)^3 \int_{-\infty}^{t} d\tau_3 \int_{-\infty}^{\tau_3} d\tau_2 \int_{-\infty}^{\tau_2} d\tau_1 \langle\langle V|\mathcal{G}(t-\tau_3)L_{\text{int}}(\tau_3)$$

$$\times \mathcal{G}(\tau_3-\tau_2)L_{\text{int}}(\tau_2)\mathcal{G}(\tau_2-\tau_1)L_{\text{int}}(\tau_1)|\rho(-\infty)\rangle\rangle. \tag{12}$$

Here the Green function $\mathcal{G}(\tau)$ is the formal solution of Eq. (8) in the absence of the electromagnetic field:

$$\mathcal{G}(\tau) \equiv \exp(-iL\tau). \tag{13}$$

For subsequent manipulations we shall also introduce the Green function in the frequency domain:

$$\hat{\mathcal{G}}(\omega) = -i\int_0^{\infty} d\tau \exp(i\omega\tau)\mathcal{G}(\tau) = \frac{1}{\omega - L}. \tag{14}$$

The interpretation of Eq. (12) is as follows: The system starts at $t = -\infty$ with a density matrix $\rho(-\infty)$. It then interacts three times with the electromagnetic field at times $\tau_1 \le \tau_2 \le \tau_3$. During the intervals between interactions $(\tau_2 - \tau_1, \tau_3 - \tau_2)$, it evolves in time according to $\mathcal{G}(\tau)$. Then the system evolves from time τ_3 to t through $\mathcal{G}(t - \tau_3)$. At time t we calculate the polarization. Equation (12) is the usual time-ordered expansion of the evolution operator. It will prove useful to make a transformation of time variables and define (Fig. 2)

$$\begin{aligned} t_1 &= \tau_2 - \tau_1, \\ t_2 &= \tau_3 - \tau_2, \\ t_3 &= t - \tau_3 \end{aligned} \tag{15a}$$

or

$$\begin{aligned} \tau_1 &= t - t_1 - t_2 - t_3, \\ \tau_2 &= t - t_2 - t_3, \\ \tau_3 &= t - t_3. \end{aligned} \tag{15b}$$

The new time variables t_1, t_2, and t_3 (Fig. 2) represent, respectively, the three intervals between τ_1 and τ_2, τ_2 and τ_3, and τ_3 and t. Equation (12) can then be recast in the form

$$P(\mathbf{r}, t) = (-i)^3 \int_0^{\infty} dt_1 \int_0^{\infty} dt_2 \int_0^{\infty} dt_3$$

$$\times \langle\langle V|\mathcal{G}(t_3)L_{\text{int}}(t-t_3)\mathcal{G}(t_2)L_{\text{int}}(t-t_2-t_3)$$

$$\times \mathcal{G}(t_1)L_{\text{int}}(t-t_1-t_2-t_3)|\rho(-\infty)\rangle\rangle. \tag{16}$$

On the substitution of Eqs. (4), (5), and (9b) into Eq. (16), we obtain an explicit expression for the polarization in terms of the incoming field amplitudes $E_j(t)$. $P(\mathbf{r}, t)$ can have any of the possible wave vectors $\mathbf{k}_s$ given in Eq. (1):

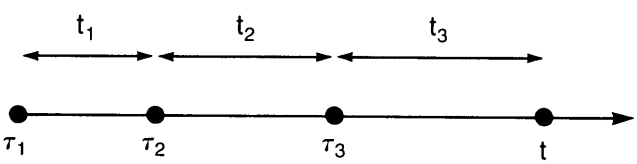

Fig. 2. The time arguments for Eqs. (12) and (16). The three radiative interactions occur at times τ_1, τ_2, and τ_3, and the nonlinear polarization is calculated at time t. These time arguments are fully ordered: $\tau_1 \le \tau_2 \le \tau_3 \le t$. t_1, t_2, and t_3 denote the time intervals between the former time arguments as indicated in Eqs. (15).

$$P(\mathbf{r}, t) = \sum_{\mathbf{k}_s,\omega_s} \exp(i\mathbf{k}_s \cdot \mathbf{r} - i\omega_s t) P(\mathbf{k}_s, t). \tag{17}$$

Hereafter, we shall select a specific choice, namely,

$$\mathbf{k}_s = \mathbf{k}_1 + \mathbf{k}_2 + \mathbf{k}_3 \tag{18a}$$

and

$$\omega_s = \omega_1 + \omega_2 + \omega_3. \tag{18b}$$

Any other combination may be obtained from our final expression by changing one (or more) $\mathbf{k}_j$ and ω_j into $-\mathbf{k}_j$ and $-\omega_j$ and $E_j(t)$ into $E_j^*(t)$. Using Eqs. (4), (5), and (16)–(18), we then get

$$P(\mathbf{k}_s, t) = (-i)^3 \sum_{m,n,q=1,2,3} \int_0^\infty dt_3 \int_0^\infty dt_2 \int_0^\infty dt_1 \times R(t_3, t_2, t_1) \exp[i(\omega_m + \omega_n + \omega_q)t_3 + i(\omega_m + \omega_n)t_2 + i\omega_m t_1] \times E_m(t - t_1 - t_2 - t_3) E_n(t - t_2 - t_3) E_q(t - t_3). \tag{19}$$

$R(t_3, t_2, t_1)$ is the *nonlinear response function*, which contains all relevant microscopic information:

$$R(t_3, t_2, t_1) \equiv \langle\langle V|\mathcal{G}(t_3)\mathcal{V}\mathcal{G}(t_2)\mathcal{V}\mathcal{G}(t_1)\mathcal{V}|\rho(-\infty)\rangle\rangle. \tag{20}$$

The summation in Eq. (19) is over all 3! = 6 permutations of the indices m, n, and q with the numbers 1, 2, and 3. Alternatively, we may define the response function in the frequency domain by performing a Fourier transform of $R(t_3, t_2, t_1)$:

$$\hat{R}(\omega_m + \omega_n + \omega_q, \omega_m + \omega_n, \omega_m) \equiv (-i)^3 \int_0^\infty dt_3 \int_0^\infty dt_2 \int_0^\infty dt_1 \times \exp[i(\omega_m + \omega_n + \omega_q)t_3 + i(\omega_m + \omega_n)t_2 + i\omega_m t_1] \times R(t_3, t_2, t_1). \tag{21}$$

Equation (19) may then be rearranged in the form

$$P(\mathbf{k}_s, t) = \sum_{m,n,q=1,2,3} \int_{-\infty}^\infty d\omega'_m \int_{-\infty}^\infty d\omega'_n \int_{-\infty}^\infty d\omega'_q \times \hat{R}(\omega'_m + \omega'_n + \omega'_q, \omega'_m + \omega'_n, \omega'_m) J_m(\omega'_m) J_n(\omega'_n) J_q(\omega'_q) \times \exp[i(\omega_m + \omega_n + \omega_q - \omega'_m - \omega'_n - \omega'_q)t], \tag{22}$$

where

$$\hat{R}(\omega_m + \omega_n + \omega_q, \omega_m + \omega_n, \omega_m) = \langle\langle V|\hat{\mathcal{G}}(\omega_m + \omega_n + \omega_q)\mathcal{V}\hat{\mathcal{G}}(\omega_m + \omega_n)\mathcal{V}\hat{\mathcal{G}}(\omega_m)\mathcal{V}|\rho(-\infty)\rangle\rangle, \tag{23}$$

and

$$J_j(\omega'_j) = (2\pi)^{-1} \int_{-\infty}^\infty d\tau E_j(\tau) \exp[i(\omega'_j - \omega_j)\tau], \qquad j = m, n, q \tag{24}$$

is the spectral density of the j field.

Equations (19) and (20) or alternatively Eqs. (22)–(24) provide the most general formal expression for any type of 4WM process.[12] The signal (field intensity) in the $\mathbf{k}_s$ direction is obtained by substituting $P(\mathbf{k}_s, t)$ as a source into the Maxwell equations and solving for the signal field. When the incident fields do not vary substantially during the process, the signal is simply proportional to the absolute square of $P(\mathbf{k}_s, t)$. We thus have for the 4WM signal in the $\mathbf{k}_s$ direction at time t (apart from some numerical and geometrical factors):

$$S(\mathbf{k}_s, t) = |P(\mathbf{k}_s, t)|^2. \tag{25}$$

Equations (19) and (20) or (22)–(24) show that the nonlinear response function $R(t_3, t_2, t_1)$ or its Fourier transform $\hat{R}(\omega_m + \omega_n + \omega_q, \omega_m + \omega_n, \omega_m)$ contains the complete microscopic information relevant to the calculation of any 4WM signal. As indicated earlier, the various 4WM techniques differ by the choice of $\mathbf{k}_s$ and ω_s and by the temporal characteristics of the incoming fields $E_1(t)$, $E_2(t)$, and $E_3(t)$. A detailed analysis of the response function and the nonlinear signal will be made in Sections 3–5 for two specific models. At this point, we shall consider the two limiting cases of ideal T4WM and S4WM. In an ideal time-domain 4WM (T4WM), the durations of the incoming fields are infinitely short, i.e.,

$$E_1(\tau) = E_1\delta(\tau - \tau^*_1),$$
$$E_2(\tau) = E_2\delta(\tau - \tau^*_2),$$
$$E_3(\tau) = E_3\delta(\tau - \tau^*_3), \tag{26}$$

where $\tau^*_1 < \tau^*_2 < \tau^*_3$. We further denote $t_1 = \tau^*_2 - \tau^*_1$, $t_2 = \tau^*_3 - \tau^*_2$, and $t_3 = t - \tau^*_3$. On the substitution of Eqs. (26) into Eq. (19) we get

$$P_s(\mathbf{k}_s, t) = E_1E_2E_3R(t_3, t_2, t_1)\exp[i\omega_1 t_1 + i(\omega_1 + \omega_2)t_2 + i(\omega_1 + \omega_2 + \omega_3)t_3] \tag{27}$$

and

$$S(\mathbf{k}_s, t) = |E_1E_2E_3|^2 |R(t_3, t_2, t_1)|^2. \tag{28}$$

The other extreme limit of 4WM is a stationary frequency-domain experiment (S4WM) in which the field amplitudes $E_1(\tau)$, $E_2(\tau)$, and $E_3(\tau)$ are time independent. In this case we have

$$J_1(\omega'_1) = E_1\delta(\omega'_1 - \omega_1),$$
$$J_2(\omega'_2) = E_2\delta(\omega'_2 - \omega_2),$$
$$J_3(\omega'_3) = E_3\delta(\omega'_3 - \omega_3). \tag{29}$$

Using Eqs. (22) and (29), we get

$$P(\mathbf{k}_s, t) = \chi^{(3)}(-\omega_s, \omega_1, \omega_2, \omega_3)E_1E_2E_3, \tag{30}$$

where the nonlinear susceptibility $\chi^{(3)}$ is given by

$$\chi^{(3)}(-\omega_s, \omega_1, \omega_2, \omega_3) = \sum_{m,n,q=1,2,3} \hat{R}(\omega_m + \omega_n + \omega_q, \omega_m + \omega_n, \omega_m). \tag{31}$$

The stationary signal [Eq. (25)] is given in this case by

$$S(\mathbf{k}_s) = |E_1E_2E_3|^2 |\chi^{(3)}(-\omega_s, \omega_1, \omega_2, \omega_3)|^2. \tag{32}$$

3. A MOLECULAR MODEL FOR THE NONLINEAR RESPONSE FUNCTION: THE OPTICAL BLOCH EQUATIONS

In order to gain a better insight into the significance of the nonlinear response function [Eq. (20) or (23)], we shall now consider a specific model system commonly used in molecu-

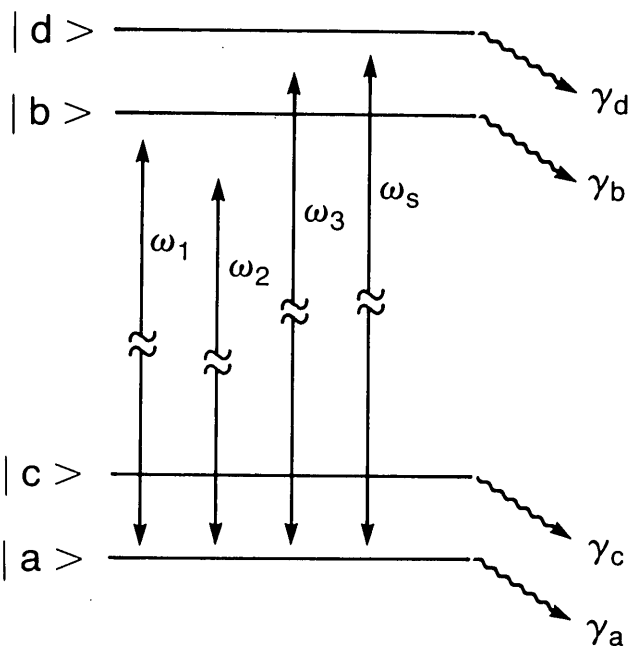

Fig. 3. The molecular level scheme and laser frequencies for 4WM. Levels $|a\rangle$ and $|c\rangle$ are part of the ground-state vibrational manifold, whereas levels $|b\rangle$ and $|d\rangle$ belong to an electronically excited manifold. γ_ν is the inverse lifetime of level $|\nu\rangle$. The electronic-dipole operator [Eq. (34)] couples vibronic states belonging to different electronic states.

lar 4WM. We consider a molecular level scheme for the absorber consisting of a manifold of vibronic levels belonging to the ground electronic state denoted $|a\rangle, |c\rangle, \ldots$, and a manifold of vibronic levels belonging to an excited electronic state denoted $|b\rangle, |d\rangle, \ldots$ (Fig. 3). The absorber is further coupled to a thermal bath, and the Hamiltonian for the nonlinear medium is

$$H = H_S + H_{SB}, \tag{33a}$$

$$H_S = \sum_{\nu=a,b,c,d\ldots} |\nu\rangle\left(\epsilon_\nu - \frac{i}{2}\gamma_\nu\right)\langle\nu|, \tag{33b}$$

$$H_{SB} = \sum_{\nu=a,b,c,d\ldots} |\nu\rangle H^\nu_{SB}(Q_B)\langle\nu|. \tag{33c}$$

Here ϵ_ν is the energy and γ_ν is the inverse lifetime of the $|\nu\rangle$ level. H is decomposed into a system Hamiltonian H_S and a system–bath Hamiltonian H^ν_{SB}, which is taken to be diagonal in the system states $|\nu\rangle$. The bath coordinates are denoted Q_B. The electronic-dipole operator of the absorber couples vibronic states belonging to different electronic states. We then have

$$V = \sum_{a,b,c,d} (\mu_{ab}|a\rangle\langle b| + \mu_{ad}|a\rangle\langle d| + \mu_{cb}|c\rangle\langle b| + \mu_{cd}|c\rangle\langle d| + \text{H.c.}), \tag{34}$$

where the summation runs over the entire manifolds of ground and electronically excited states. The molecule is taken to be initially at thermal equilibrium in the ground-state manifold, i.e.,

$$\rho(-\infty) = \sum_a |a\rangle P(a)\langle a|, \tag{35}$$

or, in Liouville-space notation,

$$|\rho(-\infty)\rangle\rangle = \sum_a P(a)|aa\rangle\rangle, \tag{36}$$

where

$$P(a) = \exp(-\beta\epsilon_a)\Big/\sum_a \exp(-\beta\epsilon_a). \tag{37}$$

In order to calculate the response function [Eq. (20)] we need the matrix elements of the absorber's Green function [Eq. (13)]. Since our Hamiltonian H [Eqs. (33)] is diagonal in the absorber states, we simply have

$$\langle\langle\nu'\lambda'|\mathcal{G}(t)|\nu\lambda\rangle\rangle_s = \langle\langle\nu\lambda|\mathcal{G}(t)|\nu\lambda\rangle\rangle_s\delta_{\nu\nu'}\delta_{\lambda\lambda'}, \tag{38a}$$

where

$$\langle\langle\nu\lambda|\mathcal{G}(t)|\nu\lambda\rangle\rangle_s = \exp[-i\omega_{\nu\lambda}t - (1/2)(\gamma_\nu + \gamma_\lambda)t] \times \langle\langle\nu\lambda|\exp(-iL_{SB}t)|\nu\lambda\rangle\rangle_s,$$

$$\nu,\lambda = a, b, c, d \ldots, \tag{38b}$$

$$\omega_{\nu\lambda} \equiv \epsilon_\nu - \epsilon_\lambda. \tag{39}$$

The action of the Liouville operator L_{SB} on an operator A is given by

$$L_{SB}A \equiv [H_{SB}, A]. \tag{40}$$

The subscript s in Eqs. (38) indicates that the matrix element involves a partial trace over the system (absorber) degrees of freedom, and $\langle\langle\nu\lambda|G(t)|\nu\lambda\rangle\rangle_s$ is still a Liouville-space operator in the bath degrees of freedom. In general, Eqs. (38) should be substituted into Eq. (20), and the resulting expression should be averaged over the bath degrees of freedom. In this section, we shall adopt the Bloch equations to account for the bath. In the absence of a radiation field, the Bloch equations for $\bar{\rho}$, the density matrix averaged over the bath degrees of freedom, are

$$\frac{d\bar{\rho}_{\nu\lambda}}{dt} = (-i\omega_{\nu\lambda} - \Gamma_{\nu\lambda})\bar{\rho}_{\nu\lambda}, \qquad \nu,\lambda = a, b, c, d \ldots, \tag{41a}$$

where

$$\bar{\rho} \equiv \mathrm{Tr}_B(\rho) \tag{41b}$$

and

$$\Gamma_{\nu\lambda} = \tfrac{1}{2}(\gamma_\nu + \gamma_\lambda) + \hat{\Gamma}_{\nu\lambda}. \tag{41c}$$

The pure dephasing rate $\hat{\Gamma}_{\nu\lambda}$ is the only effect of the bath in this approximation. The bath does not affect populations, i.e., $\hat{\Gamma}_{\nu\nu} = 0$. Typically, if ν and λ belong to two different electronic states (e.g., $\nu\lambda = ab$), then the pure-dephasing rate is much larger than if they belong to the same electronic state (e.g., $\nu\lambda = ac$). The solution of Eq. (41a) is

$$\bar{\rho}_{\nu\lambda}(t) = \langle\langle\nu\lambda|\mathcal{G}(t)|\nu\lambda\rangle\rangle\bar{\rho}_{\nu\lambda}(0), \tag{42a}$$

where the double brackets now denote a total trace (over the system and the bath), i.e.,

$$\langle\langle\nu\lambda|\mathcal{G}(t)|\nu\lambda\rangle\rangle \equiv \mathrm{Tr}_B\langle\langle\nu\lambda|\mathcal{G}(t)|\nu\lambda\rangle\rangle_s. \tag{42b}$$

The optical Bloch equations hold when the correlation time of the bath is very short compared with the time scale of the

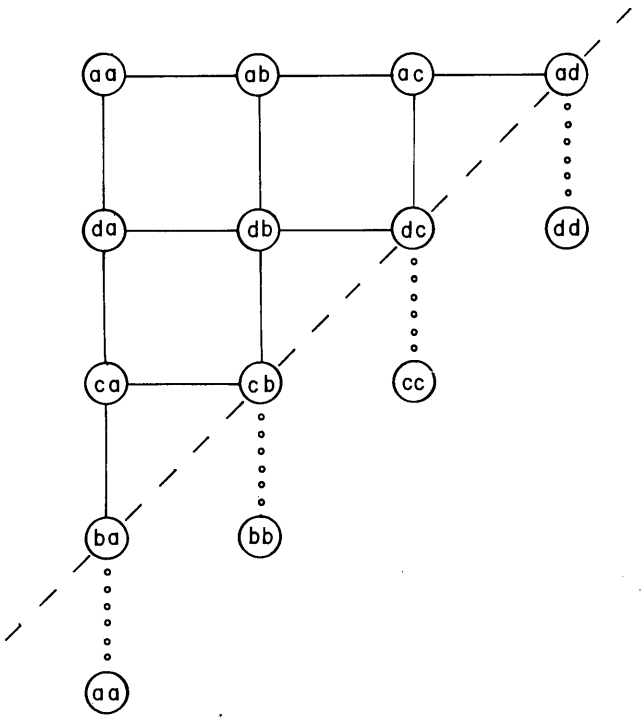

Fig. 4. Pictorial representation of the possible Liouville-space pathways[12] that contribute to the nonlinear response function [Eq. (20)]. Solid lines denote radiative coupling V. Horizontal (vertical) lines represent action of V from the right (left). Starting at aa, after three perturbations the system finds itself along the dashed line. The dotted lines represent the last V, which acts from the left. At the end of four perturbations, the system is in a diagonal state (aa, bb, cc, or dd). There are, respectively, 1, 1, 3, and 3 three-bond pathways leading to aa, ba, dc, and cb. Altogether, there are therefore eight pathways. In each pathway each of the three fields acts once.

absorber dynamics. Under these conditions, the average of the product of Green functions in Eq. (20) may be factorized into the product of the averaged Green functions [Eq. (42b)]. Making use of the factorization approximation,[12,33] we may replace $\langle\langle\nu\lambda|\mathcal{G}(t)|\nu\lambda\rangle\rangle_s$ in Eqs. (38) by its ensemble average over the bath, which we denote $I_{\nu\lambda}(t)$:

$$I_{\nu\lambda}(t) \equiv \langle\langle\nu\lambda|\mathcal{G}(t)|\nu\lambda\rangle\rangle = \exp[(i\omega_{\nu\lambda} - \Gamma_{\nu\lambda})t]. \quad (43)$$

For subsequent manipulations we shall also introduce $\hat{I}_{\nu\lambda}$ in the frequency domain:

$$\hat{I}_{\nu\lambda}(\omega) \equiv \langle\langle\nu\lambda|\hat{\mathcal{G}}(\omega)|\nu\lambda\rangle\rangle = -i\int_0^\infty d\tau I_{\nu\lambda}(\tau)\exp(i\omega\tau). \quad (44)$$

Using Eqs. (43) and (44), we get

$$\hat{I}_{\nu\lambda}(\omega) = \frac{1}{\omega - \omega_{\nu\lambda} + i\Gamma_{\nu\lambda}}. \quad (45)$$

We are now in a position to calculate the nonlinear response function $R(t_3, t_2, t_1)$ [Eq. (20)] for the present model system. The radiative interaction $\mathcal{V}$ is a commutator that can act either from the left or from the right, and its matrix elements are

$$\langle\langle\nu'\lambda'|\mathcal{V}|\nu\lambda\rangle\rangle = V_{\nu'\nu}\delta_{\lambda'\lambda} - V^*_{\lambda'\lambda}\delta_{\nu'\nu}. \quad (46)$$

The first and second terms in Eq. (46) correspond, respectively, to action of V from the left and from the right. Since Eq. (20) contains three factors of the radiative interaction $\mathcal{V}$, it will have $2^3 = 8$ terms corresponding to the various possible choices of the $\mathcal{V}$'s to act from the left or the right.[12] A pictorial representation of Eq. (20) is given in Fig. 4. We start at $|\rho(-\infty)\rangle\rangle = |aa\rangle\rangle$, which is in the upper left-hand corner. A horizontal (vertical) bond represents an interaction $\mathcal{V}$ acting from the right (left). After the first interaction (which takes place at time $t - t_1 - t_2 - t_3$), the system finds itself in either of the states $|ab\rangle\rangle$ or $|da\rangle\rangle$ (note that b and d are indices that run over the entire excited-state manifold). The system then evolves for a period t_1, interacts again (at time $t - t_2 - t_3$), evolves for a period t_2, interacts again at time $t - t_3$, and evolves for a period t_3. Then, at time t, the polarization is calculated by operating with V from the left and performing a trace. The eight pathways in Fig. 4 that contribute to R are displayed in Fig. 5. Making use of Eqs. (20), (35), (43), and (46) and Figs. 4 and 5, we obtain the nonlinear response function

$$\begin{aligned} R(t_3, t_2, t_1) = \sum_{a,b,c,d} P(a)\mu_{ab}\mu_{bc}\mu_{cd}\mu_{da}[&-I_{ad}(t_3)I_{ac}(t_2)I_{ab}(t_1) \\ &+ I_{dc}(t_3)I_{db}(t_2)I_{da}(t_1) + I_{dc}(t_3)I_{db}(t_2)I_{ab}(t_1) \\ &+ I_{dc}(t_3)I_{ac}(t_2)I_{ab}(t_1) + I_{ba}(t_3)I_{ca}(t_2)I_{da}(t_1) \\ &- I_{cb}(t_3)I_{db}(t_2)I_{ab}(t_1) - I_{cb}(t_3)I_{db}(t_2)I_{da}(t_1) \\ &- I_{cb}(t_3)I_{ca}(t_2)I_{da}(t_1)], \end{aligned} \quad (47)$$

where the eight terms correspond to the pathways (i)–(viii) of Fig. 5, respectively. Alternatively, making use of Eqs. (23), (44), and (45), we obtain the nonlinear response function in the frequency domain[12]

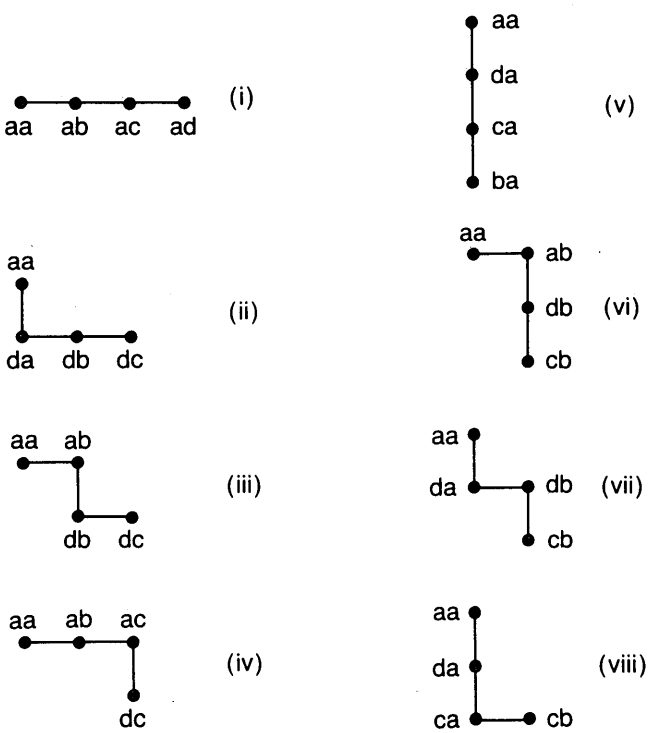

Fig. 5. The eight distinct Liouville-space pathways that contribute to the nonlinear response function [Eq. (20) or (23)]. The eight terms in Eqs. (47), (48), (53a), and (58a) correspond, respectively, to pathways (i)–(viii).

$$\hat{R}(\omega_1+\omega_2+\omega_3,\omega_1+\omega_2,\omega_1)=\sum_{a,b,c,d}P(a)\mu_{ab}\mu_{bc}\mu_{cd}\mu_{da}$$
$$\times[-\hat{I}_{ad}(\omega_1+\omega_2+\omega_3)\hat{I}_{ac}(\omega_1+\omega_2)\hat{I}_{ab}(\omega_1)$$
$$+\hat{I}_{dc}(\omega_1+\omega_2+\omega_3)\hat{I}_{db}(\omega_1+\omega_2)\hat{I}_{da}(\omega_1)$$
$$+\hat{I}_{dc}(\omega_1+\omega_2+\omega_3)\hat{I}_{db}(\omega_1+\omega_2)\hat{I}_{ab}(\omega_1)$$
$$+\hat{I}_{dc}(\omega_1+\omega_2+\omega_3)\hat{I}_{ac}(\omega_1+\omega_2)\hat{I}_{ab}(\omega_1)$$
$$+\hat{I}_{ba}(\omega_1+\omega_2+\omega_3)\hat{I}_{ca}(\omega_1+\omega_2)\hat{I}_{da}(\omega_1)$$
$$-\hat{I}_{cb}(\omega_1+\omega_2+\omega_3)\hat{I}_{db}(\omega_1+\omega_2)\hat{I}_{ab}(\omega_1)$$
$$-\hat{I}_{cb}(\omega_1+\omega_2+\omega_3)\hat{I}_{db}(\omega_1+\omega_2)\hat{I}_{da}(\omega_1)$$
$$-\hat{I}_{cb}(\omega_1+\omega_2+\omega_3)\hat{I}_{ca}(\omega_1+\omega_2)\hat{I}_{da}(\omega_1)]. \quad (48)$$

Here again, the eight terms correspond, respectively, to the pathways (i)–(viii) of Fig. 5. In concluding this section, we note that the nonlinear response function $\{R(t_3, t_2, t_1)$ [Eq. (47)] or $\hat{R}(\omega_1+\omega_2+\omega_3, \omega_1+\omega_2, \omega_1)$ [Eq. (48)]$\}$ is the fundamental quantity that contains all the relevant microscopic information for any 4WM process. Ideal T4WM probes $|R(t_3, t_2, t_1)|^2$ directly [Eq. (28)]. The response function contains eight terms that correspond to the eight distinct pathways in Liouville space (Fig. 5). S4WM is described by $\chi^{(3)}$ [Eq. (31)], which has $6 \times 8 = 48$ terms corresponding to the $3! = 6$ permutations of the time ordering of the three fields that can be made for each of the eight pathways.[5,12] In T4WM we have fewer terms than in S4WM, since in the former we can control the relative order in time of the interactions with the three fields, whereas in S4WM all orderings contribute equally to the signal. In some 4WM techniques there is a simple Fourier-transform relation between S4WM and T4WM. In other cases, however, the S4WM contains some interesting interference effects between the various time orderings that complicate the signal. Such an example (probing ground- and excited-state vibrational resonances with CARS) will be discussed in Section 5.

4. THE NONLINEAR RESPONSE FUNCTION BEYOND THE OPTICAL BLOCH EQUATIONS—A STOCHASTIC MODEL

In the previous section, we calculated the nonlinear response function $R(t_3, t_2, t_1)$ [Eq. (47)] for a model system of noninteracting multilevel absorbers. The influence of the environment on the absorbers (e.g., interactions with nonabsorbing solvent molecules in a solution or with lattice vibrations in a solid) is taken into account by using the optical Bloch equations. This amounts to adding a pure dephasing rate $\hat{\Gamma}$ to the Liouville equation [Eqs. (41)–(43)]. This approximation is justified whenever the typical correlation time associated with the bath degrees of freedom is much shorter than the time scales associated with the dynamics of the absorber. Although the Bloch equations have proved extremely useful in analyzing a wide range of nonlinear optical phenomena,[1–4] there are numerous situations in which the assumption of the separation of time scales on which they are based does not hold. For example, excited-state dynamics in large dye molecules in solutions or polymer films have been demonstrated to occur on short time scales that may be comparable to the time scale associated with solvent dynamics.[11,34] Another common situation in which the Bloch equations do not hold is pressure broadening in the gas phase at large detunings (the quasi-static limit).[33,35,36] Much insight can be gained into the effects of a bath with a finite time scale from the analysis of stochastic models that were first introduced in the context of absorption line shapes.[37–39] Such models have since been extended to the study of two-photon processes[40,41] coherent transients,[17,42,43] and 4WM.[12] Stochastic models for the bath are simpler to analyze than complete dynamical models, and, for noninteracting absorbers, they are usually exactly solvable for any correlation time of the bath. Such models interpolate between the limits of homogeneous line broadening (fast modulation of the transition energy) and inhomogeneous line broadening (a static distribution of transition energies).

In this section, we propose a stochastic model for the bath and calculate the exact nonlinear response function $R(t_3, t_2, t_1)$ for this model. As in Section 3, we consider a model in which each molecule has a manifold of vibronic states belonging to the ground electronic state labeled $|a\rangle, |c\rangle, \ldots$ and a manifold of vibronic states belonging to an excited electronic state labeled $|b\rangle, |d\rangle, \ldots$ (Fig. 3). The Hamiltonian of the system and bath [see Eqs. (33)] is given by

$$H=\sum_{\nu=a,b,c,d}|\nu\rangle[\epsilon_\nu-(i/2)\gamma_\nu+\Delta_\nu(t)]\langle\nu|, \quad (49a)$$

where

$$\Delta_\nu(t)=0, \qquad \nu=a,c,\ldots \quad (49b)$$

and

$$\Delta_\nu(t)=\Delta(t), \qquad \nu=b,d,\ldots. \quad (49c)$$

In Eq. (49), $\Delta(t)$ is the stochastic modulation of the electronic transition by interactions with the bath. $\Delta(t)$ is assumed to be a Gaussian–Markov process obeying[37–39]

$$\langle\Delta(t)\rangle=0, \quad (50a)$$

$$\langle\Delta(t_1)\Delta(t_2)\rangle=D^2\exp(-\Lambda|t_1-t_2|). \quad (50b)$$

The angle brackets in Eqs. (50) denote an average over the stochastic process. D is the root-mean-squared amplitude, and Λ^{-1} is the correlation time of the bath fluctuations. The absorber is coupled to the applied fields by the electric-dipole interaction [Eq. (34)]. Equations (49) can be obtained from our microscopic model [Eqs. (33)] by taking the bath degrees of freedom to be classical and by assuming that the bath is sufficiently large that its motions are independent of the absorber. By going to the interaction picture (with respect to the bath Hamiltonian) we may then recast Eqs. (33) in the form of Eqs. (49). The Gaussian nature of $\Delta(t)$ can be often justified by using the central-limit theorem. The choice [Eqs. (49b) and (49c)] of $\Delta_\nu(t)$ is based on the assumption that the bath couples mainly to the electronic degrees of freedom so that the ground-state and the excited-state manifolds are being stochastically modulated with respect to each other, but no modulation occurs for frequencies of levels belonging to the same electronic manifold. This is often a realistic assumption. The nonlinear response function can be evaluated also for a more general model in which each $\Delta_\nu(t)$ is an independent stochastic process.[12] However, for the sake of simplicity, we shall restrict the present discussion to this special case.

To calculate the nonlinear response function for this model, we begin with Eq. (20). Since our Hamiltonian [Eqs.

(49)] is now time dependent, we need to modify Eq. (20) slightly. It should be recast in the form

$$R(t_3, t_2, t_1) = \langle\langle V|\tilde{\mathcal{G}}(t_1 + t_2 + t_3, t_1 + t_2) \times \mathcal{V}\tilde{\mathcal{G}}(t_1 + t_2, t_1)\mathcal{V}\tilde{\mathcal{G}}(t_1, 0)\mathcal{V}|\rho(-\infty)\rangle\rangle, \quad (51)$$

where $\tilde{\mathcal{G}}(\tau_2, \tau_1)$ is the molecular evolution operator from time τ_1 to time τ_2

$$\langle\langle \nu\lambda|\tilde{\mathcal{G}}(\tau_2, \tau_1)|\nu\lambda\rangle\rangle_s = \exp\left\{-i\omega_{\nu\lambda}(\tau_2 - \tau_1) - \tfrac{1}{2}(\gamma_\nu + \gamma_\lambda)(\tau_2 - \tau_1) - i\int_{\tau_1}^{\tau_2} d\tau[\Delta_\nu(\tau) - \Delta_\lambda(\tau)]\right\} \quad (52a)$$

and

$$\langle\langle \nu'\lambda'|\tilde{\mathcal{G}}(\tau_2, \tau_1)|\nu\lambda\rangle\rangle_s = \delta_{\nu\nu'}\delta_{\lambda\lambda'}\langle\langle \nu\lambda|\tilde{\mathcal{G}}(\tau_2, \tau_1)|\nu\lambda\rangle\rangle_s. \quad (52b)$$

Of course, for a time-independent Hamiltonian, $\tilde{\mathcal{G}}(\tau_2, \tau_1)$ reduces to $\mathcal{G}(\tau_2 - \tau_1)$ [Eq. (13)], and Eq. (51) reduces to Eq. (20). The trace in Eq. (51) should now be understood to include an average over the stochastic process. Note that calculating the response function [Eq. (51)] involves averaging the product of three Green functions over the thermal bath. The Bloch-equation approximation involves the factorization of this average into the product of three averaged Green functions [Eq. (43)].[33] Our present calculation will allow us to explore the significance of this approximation. Making use of Eqs. (34) and (49)–(52), we get

$$\begin{aligned} R(t_3, t_2, t_1) = \sum_{a,b,c,d} P(a)\mu_{ab}\mu_{bc}\mu_{cd}\mu_{da} \\ \times [-K_{ad}(t_3)K_{ac}(t_2)K_{ab}(t_1)\Phi^-(t_3, t_2, t_1) \\ + K_{dc}(t_3)K_{db}(t_2)K_{da}(t_1)\Phi^-(t_3, t_2, t_1) \\ + K_{dc}(t_3)K_{db}(t_2)K_{ab}(t_1)\Phi^+(t_3, t_2, t_1) \\ + K_{dc}(t_3)K_{ac}(t_2)K_{ab}(t_1)\Phi^+(t_3, t_2, t_1) \\ + K_{ba}(t_3)K_{ca}(t_2)K_{da}(t_1)\Phi^-(t_3, t_2, t_1) \\ - K_{cb}(t_3)K_{db}(t_2)K_{ab}(t_1)\Phi^-(t_3, t_2, t_1) \\ - K_{cb}(t_3)K_{db}(t_2)K_{da}(t_1)\Phi^+(t_3, t_2, t_1) \\ - K_{cb}(t_3)K_{ca}(t_2)K_{da}(t_1)\Phi^+(t_3, t_2, t_1)], \end{aligned} \quad (53a)$$

where

$$K_{\nu\lambda}(t) = \exp[-i\omega_{\nu\lambda}t - \tfrac{1}{2}(\gamma_\nu + \gamma_\lambda)t], \quad (53b)$$

$$\Phi^\pm(t_3, t_2, t_1) = \exp\{-g(t_3) - g(t_1) \pm [g(t_1 + t_2 + t_3) + g(t_2) - g(t_1 + t_2) - g(t_2 + t_3)]\}, \quad (53c)$$

$$g(t) = \int_0^t d\tau_1 \int_0^{\tau_1} d\tau_2 \langle\Delta(\tau_1)\Delta(\tau_2)\rangle = \frac{D^2}{\Lambda^2}[\exp(-\Lambda t) - 1 + \Lambda t]. \quad (53d)$$

The functions $\Phi^\pm$ are defined by

$$\Phi^{(\pm)}(t_3, t_2, t_1) = \left\langle \exp\left[-i\int_{t_1+t_2}^{t_1+t_2+t_3} d\tau\Delta(\tau) \pm i\int_0^{t_1} d\tau\Delta(\tau)\right]\right\rangle, \quad (54)$$

where the angle brackets denote averaging over the stochastic process $\Delta(\tau)$. The average in Eq. (54) was evaluated by using the cumulant expansion (which is exact to second order for the present Gaussian–Markov model). Equation (53) should be compared with Eq. (47), which gives $R(t_3, t_2, t_1)$ for the Bloch-equation model of Section 3. The eight terms in Eq. (53a) correspond to the eight pathways of Fig. 5, respectively. Each term in Eq. (47) is a product of a function of t_1, a function of t_2, and a function of t_3. R has this structure because, in the Bloch-equation approximation, the average of the product of three Green functions in Eq. (51) factors into the product of three averaged Green functions. For a bath of arbitrary time scale, this factorization approximation no longer holds, as can be seen from Eq. (53a). Let us consider two limiting cases of Eqs. (53). In the limit of fast modulation ($\Lambda/D \gg 1$), Eq. (53c) becomes

$$\Phi^\pm(t_3, t_2, t_1) = \exp[-\hat{\Gamma}(t_3 + t_1)], \quad (55a)$$

where

$$\hat{\Gamma} = D^2/\Lambda. \quad (55b)$$

If this result is substituted into Eq. (53a), we recover the Bloch-equation result of Section 3 [Eq. (47)]. In this limit, the line-shape function $I_{\nu\lambda}$ of Eq. (43) is related to $K_{\nu\lambda}(t)$ of Eqs. (53) by

$$I_{\nu\lambda}(t) = \exp(-\hat{\Gamma}t)K_{\nu\lambda}(t). \quad (56)$$

In the limit of slow modulation ($\Lambda/D \ll 1$), Eq. (53c) becomes

$$\Phi^{(\pm)}(t_3, t_2, t_1) = \exp[-(D^2/2)(t_3 \pm t_1)^2]. \quad (57)$$

Substitution of Eq. (57) into Eqs. (53) gives the nonlinear response function of a system with a static Gaussian distribution of electronic transition frequencies (inhomogeneous line broadening).

Making use of Eqs. (53) and (21), we can evaluate the response function in the frequency domain

$$\begin{aligned} \hat{R}(\omega_1 + \omega_2 + \omega_3, \omega_1 + \omega_2, \omega_1) = \sum_{a,b,c,d} P(a)\mu_{ab}\mu_{bc}\mu_{cd}\mu_{da} \\ [-\psi^-(s_3 + \Omega_{ad}, s_2 + \Omega_{ac}, s_1 + \Omega_{ab}) \\ + \psi^-(s_3 + \Omega_{dc}, s_2 + \Omega_{db}, s_1 + \Omega_{da}) \\ + \psi^+(s_3 + \Omega_{dc}, s_2 + \Omega_{db}, s_1 + \Omega_{ab}) \\ + \psi^+(s_3 + \Omega_{dc}, s_2 + \Omega_{ac}, s_1 + \Omega_{ab}) \\ + \psi^-(s_3 + \Omega_{ba}, s_2 + \Omega_{ca}, s_1 + \Omega_{da}) \\ - \psi^-(s_3 + \Omega_{cb}, s_2 + \Omega_{db}, s_1 + \Omega_{ab}) \\ - \psi^+(s_3 + \Omega_{cb}, s_2 + \Omega_{db}, s_1 + \Omega_{da}) \\ - \psi^+(s_3 + \Omega_{cb}, s_2 + \Omega_{ca}, s_1 + \Omega_{da})], \end{aligned} \quad (58a)$$

where

$$s_1 = -i\omega_1, \quad (58b)$$

$$s_2 = -i(\omega_1 + \omega_2), \quad (58c)$$

$$s_3 = -i(\omega_1 + \omega_2 + \omega_3), \quad (58d)$$

$$\Omega_{\nu\lambda} = i\omega_{\nu\lambda} + (1/2)(\gamma_\nu + \gamma_\lambda). \quad (58e)$$

The functions $\psi^\pm$ are defined as follows:

$$\psi^{\pm}(s_3, s_2, s_1) = \int_0^\infty dt_3 \int_0^\infty dt_2 \int_0^\infty dt_1 \times \exp[-s_1 t_1 - s_2 t_2 - s_3 t_3]\phi^{\pm}(t_3, t_2, t_1). \quad (59)$$

In Appendix A, we outline a convenient computational method for evaluating this triple integral using a simple recursive formula.[40,41] Note that $\chi^{(3)}$ may be obtained by simply permuting the frequency factors in $\hat{R}$, according to Eq. (31).

There is currently great interest in the application of 4WM to obtain dynamical information from systems whose absorption line shape is dominated by static inhomogeneous broadening.[10,11,14–17,28,34,44] The information content of 4WM observables is usually established on the basis of the Bloch equations. The more general model of this section can be used to gain further insight into the line-narrowing capabilities of time- and frequency-resolved 4WM experiments. The information content of specific nonlinear spectroscopic observables for a system interacting with a bath of arbitrary time scale can be analyzed using the present model.

5. COHERENT RAMAN SPECTROSCOPY—GROUND-STATE VERSUS EXCITED-STATE CARS

As an example of the way in which the present work can be used to establish the relationships between T4WM and S4WM, we consider coherent Raman measurements [CARS and coherent Stokes Raman spectroscopy (CSRS)].[10,26–32,45,46] These experiments usually involve two fields (i.e., $\mathbf{k}_3 = \mathbf{k}_1$), and the signal mode is

$$\mathbf{k}_s = 2\mathbf{k}_1 - \mathbf{k}_2, \quad (60a)$$

$$\omega_s = 2\omega_1 - \omega_2. \quad (60b)$$

We shall start with an ideal S4WM and focus on $\chi^{(3)}$ [Eq. (31)]. Since two fields are equal, there are only three permutations of the frequencies (and not six). Setting ω_2 equal to $-\omega_2$ in Eq. (31) and writing the frequency permutations explicitly, we get

$$\chi^{(3)}(-\omega_s, \omega_1, -\omega_2, \omega_1) = \hat{R}(2\omega_1 - \omega_2, \omega_1 - \omega_2, \omega_1) + \hat{R}(2\omega_1 - \omega_2, \omega_1 - \omega_2, -\omega_2) + \hat{R}(2\omega_1 - \omega_2, 2\omega_1, \omega_1), \quad (61)$$

where $\hat{R}$ is given in Eq. (48). $\chi^{(3)}$ thus contains $3 \times 8 = 24$ terms. In CARS we look for two-photon resonances in the signal that occur when $\omega_1 - \omega_2$ equals an energy difference between two ground-state or excited-state vibrational states. For our level scheme (Fig. 3) such resonances occur for $\omega_1 - \omega_2 = \pm\omega_{ca}$ or for $\omega_1 - \omega_2 = \pm\omega_{db}$. The labels CARS and CSRS refer to the cases in which $\omega_1 > \omega_2$ and $\omega_1 < \omega_2$, respectively. Since there are no fundamental differences between the theoretical treatments of the two, we shall focus on the CARS resonances

$$\omega_1 - \omega_2 = \omega_{ca} \quad (62a)$$

and

$$\omega_1 - \omega_2 = \omega_{db}. \quad (62b)$$

Equation (62a) represents ground-state CARS, and Eq. (62b) represents excited-state CARS. For the sake of clarity and simplicity, we shall restrict the present analysis to the optical Bloch equations (Section 3). The generalization to the stochastic model is straightforward and can be made by replacing each of the relevant terms in Eq. (48) by its counterpart in Eqs. (58). From Eq. (48) it is clear that CARS resonances [Eqs. (62)] can come only from the middle Green function. We shall thus consider only the terms containing $I_{ca}(\omega_1 - \omega_2)$ and $I_{db}(\omega_1 - \omega_2)$. It is also clear from Eq. (61) that the third term $\hat{R}(2\omega_1 - \omega_2, 2\omega_1, \omega_1)$ cannot contribute to CARS, since its two-photon resonances are at $2\omega_1$ and not at $\omega_1 - \omega_2$. We shall therefore ignore this term. Let us denote the eight diagrams of the first term in Eq. (61) by (i)–(viii) and the corresponding ones for the second term in Eq. (61) by $(i)'$ ... (viii)′ (see Fig. 5). Starting with ground-state CARS, we note that there are four terms containing $I_{ca}(\omega_1 - \omega_2)$. These correspond to diagrams (v), (viii), (v)′, and (viii)′, i.e.,

$$\chi_{ca}^{(3)} = \sum_{b,d} P(a)\mu_{ab}\mu_{bc}\mu_{cd}\mu_{da}[\hat{I}_{ba}(2\omega_1 - \omega_2)\hat{I}_{ca}(\omega_1 - \omega_2) - \hat{I}_{cb}(2\omega_1 - \omega_2)\hat{I}_{ca}(\omega_1 - \omega_2)] \times [\hat{I}_{da}(\omega_1) + \hat{I}_{da}(-\omega_2)], \quad (63)$$

where the subscript in χ_{ca} denotes that these are ground-state ($\omega_1 - \omega_2 = \omega_{ca}$) resonances. We shall now invoke the rotating-wave approximation (RWA) in which we retain only resonant terms, in which all denominators contain a difference of a field frequency and a molecular optical frequency, and neglect all terms in which at least one denominator is antiresonant. For the ground-state CARS, the only term that survives is diagram (v):

$$\chi_{ca}^{(3)} = \sum_{b,d} P(a)\mu_{ab}\mu_{bc}\mu_{cd}\mu_{da}\hat{I}_{ba}(2\omega_1 - \omega_2)\hat{I}_{ca}(\omega_1 - \omega_2)\hat{I}_{da}(\omega_1). \quad (64)$$

Similarly, for the excited-state CARS we have eight terms in Eq. (61) that contain $\hat{I}_{db}(\omega_1 - \omega_2)$. These correspond to pathways (ii), (iii), (vi), and (vii) and (ii)′, (iii)′, (vi)′, and (vii)′:

$$\chi_{db}^{(3)} = \sum_{a,c} P(a)\mu_{ab}\mu_{bc}\mu_{cd}\mu_{da}[\hat{I}_{dc}(2\omega_1 - \omega_2)\hat{I}_{db}(\omega_1 - \omega_2) - \hat{I}_{cb}(2\omega_1 - \omega_2)\hat{I}_{db}(\omega_1 - \omega_2)] \times [\hat{I}_{da}(\omega_1) + \hat{I}_{da}(-\omega_2) + \hat{I}_{ab}(\omega_1) + \hat{I}_{ab}(-\omega_2)]. \quad (65)$$

Within the RWA, only two terms contribute to $\chi_{db}^{(3)}$, which come from pathways (ii) and (iii)′, i.e.,

$$\chi_{db}^{(3)} = \sum_{a,c} P(a)\mu_{ab}\mu_{bc}\mu_{cd}\mu_{da} \times \hat{I}_{dc}(2\omega_1 - \omega_2)\hat{I}_{db}(\omega_1 - \omega_2)[\hat{I}_{da}(\omega_1) + \hat{I}_{ab}(-\omega_2)]. \quad (66)$$

Making use of the explicit form of $\hat{I}_{\nu\lambda}(\omega)$ [Eq. (45)] and Eqs. (64) and (66), we therefore have

$$\chi_{ca}^{(3)} = \sum_{b,d} P(a)\mu_{ab}\mu_{bc}\mu_{cd}\mu_{da} \frac{1}{2\omega_1 - \omega_2 - \omega_{ba} + i\Gamma_{ba}} \times \frac{1}{\omega_1 - \omega_2 - \omega_{ca} + i\Gamma_{ca}} \frac{1}{\omega_1 - \omega_{da} + i\Gamma_{da}} \quad (67a)$$

and

$$\chi_{db}^{(3)} = \sum_{a,c} P(a)\mu_{ab}\mu_{bc}\mu_{cd}\mu_{da} \times \frac{1}{2\omega_1 - \omega_2 - \omega_{dc} + i\Gamma_{dc}} \frac{1}{\omega_1 - \omega_2 - \omega_{db} + i\Gamma_{db}} \times \left[\frac{1}{\omega_1 - \omega_{da} + i\Gamma_{da}} + \frac{1}{-\omega_2 - \omega_{ab} + i\Gamma_{ab}}\right]. \quad (67b)$$

Equations (67) show that the excited-state CARS arises from two pathways that interfere, whereas the ground-state CARS is associated with only one pathway. To make the interference in Eq. (67b) more explicit, we rearrange it in the form

$$\chi_{db}^{(3)} = \sum_{a,c} P(a)\mu_{ab}\mu_{bc}\mu_{cd}\mu_{da} \times \frac{1}{2\omega_1 - \omega_2 - \omega_{dc} + i\Gamma_{dc}} \frac{1}{\omega_1 - \omega_{da} + i\Gamma_{da}} \times \frac{1}{-\omega_2 - \omega_{ab} + i\Gamma_{ab}}\left[1 + \frac{i\tilde{\Gamma}}{\omega_1 - \omega_2 - \omega_{db} + i\Gamma_{db}}\right], \quad (68)$$

where

$$\tilde{\Gamma} \equiv \Gamma_{ab} + \Gamma_{ad} - \Gamma_{bd} = \gamma_a + \hat{\Gamma}_{ab} + \hat{\Gamma}_{ad} - \hat{\Gamma}_{bd}. \quad (69)$$

The CARS resonance is contained in the term in Eq. (68) that is proportional to $\tilde{\Gamma}$. When $|a\rangle$ is the actual ground vibronic state, $\gamma_a = 0$, and $\tilde{\Gamma}$ is then a combination of pure-dephasing widths that vanishes in the absence of pure dephasing. The two pathways thus interfere destructively, and, in the absence of pure dephasing, the CARS excited-state resonance disappears. In the presence of pure dephasing, the cancellation is not complete, and a dephasing-induced resonance appears. Such resonances have been observed experimentally. They have been denoted PIER4 (pressure-induced extra resonance in four-wave mixing)[9] and DICE (dephasing-induced coherent emission).[10]

Equations (67) and (68) show that in S4WM there is a fundamental difference between the ground-state and the excited-state CARS resonances. The interference in Eq. (66) occurs between two pathways in which the first interaction occurs, respectively, with ω_1 and with $-\omega_2$. In a S4WM we have no control over the relative order in time of both interactions. Both pathways contribute equally, and they interfere. The situation is quite different when the CARS experiment is done in the time domain (T4WM). A time-domain CARS experiment is usually performed by sending two time-coincident pulses with wave vectors $\mathbf{k}_1$ and $\mathbf{k}_2$ into the sample. After a variable delay, T, a second $\mathbf{k}_1$ pulse is applied, and the total coherent emission at $\mathbf{k}_s = 2\mathbf{k}_1 - \mathbf{k}_2$ is detected. We shall assume that all pulses have the same shape, $E(t)$, and that the pulse duration is short compared with T. Since the last interaction has to be with ω_1, there are only two permutations of frequencies that will contribute to Eq. (19):

$$P(\mathbf{k}_s, t) = (-i)^3 \int_0^\infty dt_3 \int_0^\infty dt_2 \int_0^\infty dt_1 R(t_3, t_2, t_1) \times E(t - t_3 - T)\exp[i(2\omega_1 - \omega_2)t_3]\{E^*(t - t_2 - t_3) \times E(t - t_1 - t_2 - t_3)\exp[i\omega_1 t_1 + i(\omega_1 - \omega_2)t_2] + E(t - t_2 - t_3)E^*(t - t_1 - t_2 - t_3) \times \exp[-i\omega_2 t_1 + i(\omega_1 - \omega_2)t_2]\}. \quad (70)$$

Equation (70) is the time-domain analog of Eq. (61) and contains 16 terms. We now make the following assumptions: The pulse envelope $E(\tau)$ is sufficiently long that its spectral bandwidth is narrow enough to select a particular resonance ($\omega_1 - \omega_2 = \omega_{db}$ or $\omega_1 - \omega_2 = \omega_{ac}$). We further assume the RWA so that the same terms that contribute in the frequency domain will contribute here. On the other hand, we take the pulses to be sufficiently short that $I_{\nu\lambda}(t)$ cannot evolve appreciably during the pulses. We can therefore select the same terms that contributed to Eqs. (63) and (65) and set

$$E(\tau) = E\delta(\tau) \quad (71)$$

in Eq. (70). We then get for the ground-state CARS

$$P_{ca}(\mathbf{k}_s, t) = E^3 \sum_{a,b,c,d} P(a)\mu_{ab}\mu_{bc}\mu_{cd}\mu_{da} I_{ba}(t - T)I_{ca}(T) \times \exp[i(2\omega_1 - \omega_2)t - i\omega_1 T] \quad (72a)$$

and for the excited-state CARS

$$P_{db}(\mathbf{k}_s, t) = 2E^3 \sum_{a,b,c,d} P(a)\mu_{ab}\mu_{bc}\mu_{cd}\mu_{da} I_{dc}(t - T)I_{db}(T) \times \exp[i(2\omega_1 - \omega_2)t - i\omega_1 T]. \quad (72b)$$

The frequency-domain interference of Eq. (67b) is no longer present. The system does not have time to evolve between the first two interactions, and the two pathways that contribute to Eq. (72b) [(ii) and (iii)′] give an identical contribution. When the signal is probed as a function of T at $t = T$, we have

$$S_{ca}(T) \propto |I_{ca}(T)|^2 = \exp(-2\Gamma_{ca}T) \quad (73a)$$

and

$$S_{db}(T) \propto |I_{db}(T)|^2 = \exp(-2\Gamma_{db}T). \quad (73b)$$

The time domain CARS can be used to probe excited-state resonances even in the absence of pure dephasing, since the destructive interference of the frequency-domain CARS disappears. This point was discussed recently by Weitekamp *et al.*[32] The present analysis clarifies the origin of this difference.

6. CONCLUDING REMARKS

In this paper we developed a general theory of 4WM processes in terms of the nonlinear response function of the nonlin-

ear medium $R(t_3, t_2, t_1)$. The response function is an intrinsic molecular property that contains all the microscopic information relevant to any type of 4WM process. The details of a particular 4WM experiment are contained in the external fields, $E_1(t)$, $E_2(t)$, $E_3(t)$, and in the particular choice of the observable mode $\mathbf{k}_s$. The generated signal is calculated by convolving the response function with the external fields and choosing $\mathbf{k}_s$ [Eq. (19) or (22)]. It is only at this stage that the distinction is made among the various 4WM techniques (photon echo, transient grating, CARS, CSRS, etc.). We have shown that the response function contains eight terms (Fig. 5). We can express each term using the four-point correlation function of the dipole operator, i.e.,

$$F(\tau_1, \tau_2, \tau_3, \tau_4) \equiv \mathrm{Tr}[V(\tau_1)V(\tau_2)V(\tau_3)V(\tau_4)\rho(-\infty)] = \langle V(\tau_1)V(\tau_2)V(\tau_3)V(\tau_4)\rangle, \quad (74a)$$

where

$$V(\tau) = \exp(iH\tau)V\exp(-iH\tau). \quad (74b)$$

Here, H is the molecular Hamiltonian [Eqs. (33)], and V is the dipole operator [Eq. (34)]. In terms of this four-point correlation function, we have[12]

$$\begin{aligned} R(t_3, t_2, t_1) = &-F(0, t_1, t_1 + t_2, t_1 + t_2 + t_3) \\ &+ F(t_1, t_1 + t_2, t_1 + t_2 + t_3, 0) \\ &+ F(0, t_1 + t_2, t_1 + t_2 + t_3, t_1) \\ &+ F(0, t_1, t_1 + t_2 + t_3, t_1 + t_2) \\ &+ F(t_1 + t_2 + t_3, t_1 + t_2, t_1, 0) \\ &- F(0, t_1 + t_2 + t_3, t_1 + t_2, t_1) \\ &- F(t_1, t_1 + t_2 + t_3, t_1 + t_2, 0) \\ &- F(t_1 + t_2, t_1 + t_2 + t_3, t_1, 0), \end{aligned} \quad (75)$$

where the eight terms correspond, respectively, to diagrams (i)–(viii) of Fig. 5. It is therefore clear that the various 4WM processes probe different features of the four-point correlation function of the dipole operator. The response function discussed in this article is closely related to that introduced by Butcher.[2] Our time arguments t_1, t_2, and t_3 (Fig. 2) were chosen, however, differently. With the present choice, the relations between T4WM and S4WM are clearer. Since the response function is probing the four-point correlation function [Eqs. (74) and (75)], it necessarily contains more information than the ordinary absorption line shape that is given by the two-time correlation function $\langle V(\tau)V(0)\rangle$. This can be utilized, e.g., to eliminate inhomogeneous broadening selectively, as is done in photon echoes.[14–17] The extra resonances (PIER4, DICE)[9,10] discussed in Section 5 can be also used selectively to eliminate inhomogeneous broadening. We have evaluated R for a stochastic model for a bath with an arbitrary time scale. Our solution [Eqs. (53) or (58)] is a generalization of the results of the optical Bloch equations and reduces to that solution in the limit of fast modulation. The stochastic expression for R permits a better understanding of the interplay between homogeneous and inhomogeneous broadening in 4WM. We further note that in T4WM we may control the order in time of the various radiative interactions. In a steady-state experiment (S4WM), however, all time orderings contribute equally. The T4WM is therefore simpler, and some interesting interference effects may show up in S4WM. This was demonstrated in our discussion of ground-state and excited-state CARS in Section 5.

APPENDIX A

We wish to evaluate $\psi^{\pm}$ [Eq. (59)], which is the triple Laplace transform of $\Phi^{\pm}$ [Eq. (53c)]. Following Takagahara *et al.*[40] and Mukamel,[41] we shall first write Eq. (53c) explicitly, using Eq. (53d), as

$$\Phi^{\pm}(\tau_1, \tau_2, \tau_3) = \exp\{-g(\tau_1) - g(\tau_3) \pm \eta\exp(-\Lambda\tau_2)[1 - \exp(-\Lambda\tau_1)][1 - \exp(-\Lambda\tau_3)]\}, \quad (A1)$$

where

$$\eta = D^2/\Lambda^2. \quad (A2)$$

If we expand Eq. (A1) in a Taylor series in $\exp(-\Lambda\tau_2)$ and substitute back into Eq. (59), we can carry out the τ_2 integration resulting in

$$\psi^{\pm}(s_1, s_2, s_3) = \sum_{n=0}^{\infty} (\pm 1)^n \frac{\eta^n}{n!} \frac{1}{s_2 + n\Lambda} \tilde{J}_n(s_1)\tilde{J}_n(s_3), \quad (A3)$$

where

$$\tilde{J}_n(s) = \int_0^{\infty} d\tau[1 - \exp(-\Lambda\tau)]^n \exp[-s\tau - g(\tau)]. \quad (A4)$$

On integrating Eq. (A4) by parts, we get the recursion relations

$$\eta\Lambda\tilde{J}_{n+1}(s) = n\Lambda\tilde{J}_{n-1}(s) - (s + n\Lambda)\tilde{J}_n(s), \qquad n = 1, 2, \ldots, \quad (A5)$$

and

$$\eta\Lambda\tilde{J}_1(s) = -s\tilde{J}_0(s). \quad (A6)$$

Equations (A5) and (A6) can now be used to generate a continued fraction representation of J_0

$$\tilde{J}_0(s) = \cfrac{1}{s + \cfrac{D^2}{s + \Lambda + \cfrac{2D^2}{s + 2\Lambda + \cfrac{3D^2}{s + 3\Lambda + \ldots}}}} \quad (A7)$$

Equations (A5)–(A7) allow us to calculate $\tilde{J}_n$ recursively.

ACKNOWLEDGMENTS

The support of the National Science Foundation, the U.S. Office of Naval Research, the U.S. Army Research Office, and the donors of the Petroleum Research Fund administered by the American Chemical Society is gratefully acknowledged. We thank D. Wiersma for useful discussions. Special thanks go to June M. Rouse for the careful typing.

Shaul Mukamel is a Camille and Henry Dreyfus teacher–scholar.

REFERENCES

1. N. Bloembergen, *Nonlinear Optics* (Benjamin, New York, 1965).
2. P. N. Butcher, *Nonlinear Optical Phenomena* (Ohio U. Press, Athens, Ohio, 1965).
3. M. D. Levenson, *Introduction to Nonlinear Laser Spectroscopy* (Academic, New York, 1982).
4. Y. R. Shen, *The Principles of Nonlinear Optics* (Wiley, New York, 1984).
5. N. Bloembergen, H. Lotem, and R. T. Lynch, "Lineshapes in coherent resonant Raman scattering," Indian J. Pure Appl. Phys. **16,** 151 (1978).
6. S. A. J. Druet and J. P. E. Taran, "CARS spectroscopy," Prog. Quantum Electron. **7,** 1 (1981).
7. T. K. Lee and T. K. Gustafson, "Diagrammatic analysis of the density operator for nonlinear optical calculations: pulsed and cw responses," Phys. Rev. A **18,** 1597 (1978).
8. J. L. Oudar and Y. R. Shen, "Nonlinear spectroscopy by multiresonant four-wave mixing," Phys. Rev. A **22,** 1141 (1980).
9. Y. Prior, A. R. Bogdan, M. Dagenais, and N. Bloembergen, "Pressure-induced extra resonances in four-wave mixing," Phys. Rev. Lett. **46,** 111 (1981); A. R. Bogdan, M. W. Downer, and N. Bloembergen, "Quantitative characteristics of pressure-induced four-wave mixing signals observed with cw laser beams," Phys. Rev. A **24,** 623 (1981); L. J. Rothberg and N. Bloembergen, "High resolution four-wave light mixing studies of collision-induced coherence in Na vapor," Phys. Rev. A **30,** 820 (1984).
10. J. R. Andrews and R. M. Hochstrasser, "Thermally induced excited-state coherent Raman spectra of solids," Chem. Phys. Lett. **82,** 381 (1981); J. R. Andrews, R. M. Hochstrasser, and H. P. Trommsdorff, "Vibrational transitions in excited states of molecules using coherent Stokes Raman spectroscopy: application to ferrocytochrome-C," Chem. Phys. **62,** 87 (1981).
11. T. Yajima and H. Souma, "Study of ultra-fast relaxation processes by resonant Rayleigh-type optical mixing. I. Theory," Phys. Rev. A **17,** 309 (1978); T. Yajima, H. Souma, and Y. Ishida, "Study of ultra-fast relaxation processes by resonant Rayleigh-type optical mixing. II. Experiment on dye solutions," Phys. Rev. A **17,** 324 (1978).
12. S. Mukamel, "Non-impact unified theory of four-wave mixing and two-photon processes," Phys. Rev A **28,** 3480 (1983).
13. V. Mizrahi, Y. Prior, and S. Mukamel, "Single atom versus coherent pressure induced extra resonances in four-photon processes," Opt. Lett. **8,** 145 (1983); R. W. Boyd and S. Mukamel, "The origin of spectral holes in pump-probe studies of homogeneously broadened lines," Phys. Rev. A **29,** 1973 (1984).
14. I. D. Abella, N. A. Kurnit, and S. R. Hartmann, "Photon echoes," Phys. Rev. **141,** 391 (1966); S. R. Hartmann, "Photon, spin, and Raman echoes," IEEE J. Quantum Electron. **4,** 802 (1968); T. W. Mossberg, R. Kachru, A. M. Flusberg, and S. R. Hartmann, "Echoes in gaseous media: a generalized theory of rephasing phenomena," Phys. Rev. A **20,** 1976 (1979).
15. W. H. Hesselink and D. A. Wiersma, "Theory and experimental aspects of photon echoes in molecular solids," in *Modern Problems in Condensed Matter Sciences*, V. M. Agranovich and A. A. Maradudin, eds. (North-Holland, Amsterdam, 1983), Vol. 4, p. 249.
16. R. W. Olson, F. G. Patterson, H. W. H. Lee, and M. D. Fayer, "Delocalized electronic excitations of pentacene dimers in a p-terphenyl host: picosecond photon echo experiments," Chem. Phys. Lett. **78,** 403 (1981).
17. R. F. Loring and S. Mukamel, "Unified theory of photon echoes: the passage from inhomogeneous to homogeneous line broadening," Chem. Phys. Lett. **114,** 426 (1985).
18. J. R. Salcedo, A. E. Siegman, D. D. Dlott, and M. D. Fayer, "Dynamics of energy transport in molecular crystals: the picosecond transient grating method," Phys. Rev. Lett. **41,** 131 (1978).
19. M. D. Fayer, "Dynamics of molecules in condensed phases: picosecond holographic grating experiments," Ann. Rev. Phys. Chem. **33,** 63 (1982).
20. P. F. Liao, L. M. Humphrey, and D. M. Bloom, "Determination of upper limits for spatial energy diffusion in ruby," Phys. Rev. B **10,** 4145 (1979).
21. J. K. Tyminski, R. C. Powell, and W. K. Zwicker, "Investigation of four-wave mixing in $Nd_xLa_{1-x}P_5O_{14}$," Phys. Rev. B **29,** 6074 (1984).
22. H. J. Eichler, "Laser-induced grating phenomena," Opt. Acta **24,** 631 (1977).
23. A. von Jena and H. E. Lessing, "Theory of laser-induced amplitude and phase gratings including photoselection, orientational relaxation, and population kinetics," Opt. Quantum Electron. **11,** 419 (1979).
24. R. F. Loring and S. Mukamel, "Microscopic theory of the transient grating experiment," J. Chem. Phys. **83,** 4353 (1985); "Extra resonance in four-wave mixing as a probe of exciton dynamics: the steady-state analog of the transient grating," J. Chem. Phys. **84,** 1228 (1986).
25. N. Bloembergen, "The stimulated Raman effect," Am. J. Phys. **35,** 989 (1967).
26. A. Laubereau and W. Kaiser, "Vibrational dynamics of liquids and solids investigated by picosecond light pulses," Rev. Mod. Phys. **50,** 607 (1978); W. Zinth, H.-J. Polland, A. Laubereau, and W. Kaiser, "New results on ultrafast coherent excitation of molecular vibrations in liquids," Appl. Phys. B **26,** 77 (1981).
27. S. M. George, A. L. Harris, M. Berg, and C. B. Harris, "Picosecond studies of the temperature dependence of homogeneous and inhomogeneous linewidth broadening in liquid acetonitrile," J. Chem. Phys. **80,** 83 (1984).
28. R. F. Loring and S. Mukamel, "Selectivity in coherent transient Raman measurements of vibrational dephasing in liquids," J. Chem. Phys. **83,** 2116 (1985).
29. I. I. Abram, R. M. Hochstrasser, J. E. Kohl, M. G. Semack, and D. White, "Coherence loss for vibrational and librational excitations in solid nitrogen," J. Chem. Phys. **71,** 153 (1979); F. Ho, W. S. Tsay, J. Trout, S. Velsko, and R. M. Hochstrasser, "Picosecond time-resolved CARS in isotopically mixed crystals of benzene," Chem. Phys. Lett. **97,** 141 (1983); S. Velsko, J. Trout, and R. M. Hochstrasser, "Quantum beating of vibrational factor group components in molecular solids," J. Chem. Phys. **79,** 2114 (1983).
30. E. L. Chronister and D. D. Dlott, "Vibrational energy transfer and localization in disordered solids by picosecond CARS spectroscopy," J. Chem. Phys. **79,** 5286 (1984); C. L. Schosser and D. D. Dlott, "A picosecond CARS study of vibron dynamics in molecular crystals: temperature dependence of homogeneous and inhomogeneous linewidths," J. Chem. Phys. **80,** 1394 (1984).
31. B. H. Hesp and D. A. Wiersma, "Vibrational relaxation in neat crystals of naphthalene by picosecond CARS," Chem. Phys. Lett. **75,** 423 (1980).
32. D. P. Weitekamp, K. Duppen, and D. A. Wiersma, "Delayed four-wave mixing spectroscopy in molecular crystals: a nonperturbative approach," Phys. Rev. A **27,** 3089 (1983).
33. S. Mukamel, "Collisional broadening of spectral line shapes in two-photon and multiphoton processes," Phys. Rep. **93,** 1 (1982).
34. A. M. Weiner, S. DeSilvestri, and E. P. Ippen, "Three-pulse scattering for femtosecond dephasing studies: theory and experiment," J. Opt. Soc. Am. B **2,** 654 (1985).
35. R. G. Breene, *Theories of Spectral Line Shape* (Wiley, New York, 1981).
36. K. Burnett, "Collisional redistribution of radiation," Phys. Rep. **118,** 339 (1985).
37. N. Bloembergen, E. M. Purcell, and R. V. Pound, "Relaxation effects in nuclear magnetic resonance absorption," Phys. Rev. **73,** 679 (1948).
38. P. W. Anderson and P. R. Weiss, "Exchange narrowing in paramagnetic resonance," Rev. Mod. Phys. **25,** 269 (1953).
39. R. Kubo, "A stochastic theory of line-shape and relaxation," in *Fluctuations, Relaxation and Resonance in Magnetic Systems*," D. ter Haar, ed. (Plenum, New York, 1962), p. 23.
40. T. Takagahara, E. Hanamura, and R. Kubo, "Stochastic models of intermediate state interaction in second order optical processes—stationary response. I," J. Phys. Soc. Jpn. **43,** 802 (1977); "Stochastic models of intermediate state interaction in

second order optical processes—stationary response. II," J. Phys. Soc. Jpn. **43,** 811 (1977); "Stochastic models of intermediate state interaction in second order optical processes—transient response," J. Phys. Soc. Jpn. **43,** 1522 (1977).
41. S. Mukamel, "Stochastic theory of resonance Raman line shapes of polyatomic molecules in condensed phases," J. Chem. Phys. **82,** 5398 (1985).
42. E. Hanamura, "Stochastic theory of coherent optical transients," J. Phys. Soc. Jpn. **52,** 2258 (1983); "Stochastic theory of coherent optical transients. II. Free induction decay in Pr^{+3}: LaF_3," J. Phys. Soc. Jpn. **52,** 3678 (1983); H. Tsunetsugu, T. Taniguchi, and E. Hanamura, "Exact solution for two level electronic system with frequency modulation under laser irradiation," Solid State Commun. **52,** 663 (1984).
43. M. Aihara, "Non-Markovian theory of nonlinear optical phenomena associated with the extremely fast relaxation in condensed matter," Phys. Rev. B **25,** 53 (1982).
44. G. J. Small, "Persistent nonphotochemical hole burning and the dephasing of impurity electronic transitions in organic glasses," in *Spectroscopy and Excitation Dynamics of Condensed Molecular Systems*, V. M. Agranovich and R. M. Hochstrasser, eds. (North-Holland, New York, 1983), pp. 515; T. C. Caau, C. K. Johnson, and G. J. Small, "Multiresonant four-wave mixing spectroscopy of pentacene in naphthalene," J. Phys. Chem. **89,** 2984 (1985).
45. B. S. Hudson, W. H. Hetherington, S. P. Cramer, I. Chabay, and G. K. Klauminzer, "Resonance enhanced coherent anti-Stokes Raman scattering," Proc. Natl. Acad. Sci. (USA) **73,** 3798 (1976).
46. L. A. Carreira, T. C. Maguire, and T. B. Malloy, "Excitation profiles of the coherent anti-Stokes resonance Raman spectrum of β-carotene," J. Chem. Phys. **66,** 2621 (1977).

Shaul Mukamel

Shaul Mukamel received the Ph.D. degree in chemistry in 1976 from Tel Aviv University. Following postdoctoral research at the Massachusetts Institute of Technology and the University of California, Berkeley, he became assistant professor at Rice University in 1978. In 1981 he became associate professor at the Weizmann Institute of Science, and in 1982 he joined the faculty at the University of Rochester, where he is currently a professor of chemistry. His research interests are in molecular nonlinear optics, spectral line broadening, transport of excitations in disordered systems, molecular relaxation, and nonequilibrium statistical mechanics. He is an Alfred P. Sloan Fellow and a Camille and Henry Dreyfus teacher–scholar.

Roger F. Loring

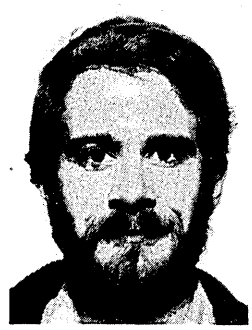

Roger F. Loring received the B.S. degree in chemistry from the University of California at Davis in 1980 and the Ph.D. degree in physical chemistry from Stanford University in 1984. He is currently a research associate in the Department of Chemistry at the University of Rochester. His research deals with excited-state dynamics of molecules in condensed phases.